ISSN 1063-7745, Crystallography Reports, 2022, Vol. 67, No. 2, pp. 278–285. © Pleiades Publishing, Inc., 2022.
Russian Text © The Author(s), 2022, published in Kristallografiya, 2022, Vol. 67, No. 2, pp. 325–332.

NANOMATERIALS AND CERAMICS

X-ray Diffraction Study of Structural Changes in High-Strength Ceramics Based on Zirconium Oxide with Additions of Ytterbium and Neodymium Oxides after Hydrothermal Treatment

V. P. Sirotinkin[a],*, L. I. Podzorova[a], N. A. Mikhailina[a], and O. I. Pen'kova[a]

[a] *Baikov Institute of Metallurgy and Materials Science, Russian Academy of Sciences, Moscow, 119334 Russia*

**e-mail: sir@imet.ac.ru*

Received October 20, 2020; revised February 28, 2021; accepted February 28, 2021

Abstract—A surface structural analysis of two ceramic samples of zirconium oxide (ZrO_2) sintered at 1550°C, stabilized in the tetragonal form, before and after hydrothermal treatment, has been performed by the Rietveld method based on X-ray diffraction (XRD) data. The first sample was zirconium oxide with addition of ytterbium oxide (3 mol %), and the second sample contained ytterbium (3 mol %) and neodymium (0.25 mol %) oxides. The hydrothermal treatment is found to change the phase composition. In the initial state, there are two tetragonal ZrO_2 forms (*t* and *t*'). The processes of surface-layer dissolution and crystallization of the monoclinic ZrO_2 modification occur during hydrothermal treatment. ZrO_2 crystals are shaped as plates elongated in the [111] direction, with developed {001} faces. Addition of neodymium oxide slows down the monoclinic-phase formation.

DOI: 10.1134/S1063774522020171

INTRODUCTION

Ceramics based on solid solutions of zirconium dioxide, stabilized in the tetragonal form, belong to the class of transformation toughened materials. Due to the polymorphic transformations in the monoclinic–tetragonal–cubic series of zirconium dioxide modifications, occurring with an increase in volume, these materials exhibit high resistance to brittle fracture. Their crack resistance coefficient reaches 20 MPa $m^{1/2}$, which is much higher than the corresponding values for ceramics of other types [1]. Currently, ceramics based on a solid solution of tetragonal zirconium dioxide, stabilized with yttrium oxide, is used in endoprosthetics of joints [2, 3] and in dental orthopedics [4]. The strength characteristics of this ceramics under long-term in vivo conditions were found to be unstable because of the change in its phase composition. This effect was referred to as low-temperature degradation [5–7]. One can eliminate it by changing the type of stabilizing cation and modifying the ceramics. In particular, the possibility of replacing zirconium with ytterbium was demonstrated in [8, 9]. According to the X-ray diffraction (XRD) data, three tetragonal ZrO_2 forms may arise at different substitutions: *t*, *t*', and *t*''; they are characterized by the same sp. gr. $P4_2/nmc$. These forms differ by the degree of distortion of the ideal cubic fluorite cell [10–12].

The purpose of this study was to determine the structure of the surface layer of ceramics based on a ZrO_2 solid solution, stabilized in the tetragonal form by adding only ytterbium oxide (3 mol % Yb_2O_3) of a mixture of neodymium and ytterbium oxides (3 mol % Yb_2O_3 and 0.25 mol % Nd_2O_3), before and after hydrothermal treatment, which imitated long-term in vivo conditions.

EXPERIMENTAL

The starting powders of two compositions (97 mol % ZrO_2, 3 mol % Yb_2O_3 and 96.75 mol % ZrO_2, 3 mol % Yb_2O_3, 0.25 mol % Nd_2O_3) were prepared by hydrolytic sol–gel synthesis. Hydrogels were precipitated simultaneously from a mixture of 1 M solutions of $ZrOCl_2$, $Yb(NO_3)_3$, and $Nd(NO_3)_3$ salts using 6 N ammonia solution, and the obtained precipitates were filtered, washed from anion residues, and dried in air at a temperature of 180°C in ethanol environment. Agents of analytical grade were used. The heat treatment of xerogels was performed at a temperature of 950°C. Preforms for sintering were pressed into disks 18 mm in diameter using semi-dry method at a specific pressure of 200 MPa. The obtained preforms were sintered at a temperature of 1550°C for 4 h in electrical furnaces in air. After sintering the samples with a relative density of no less than 98% of the theoretical value were obtained (samples 1 and 2). They were subjected to hydrothermal treatment according to the accelerated aging technique (ISO 13356-2008) under the fol-

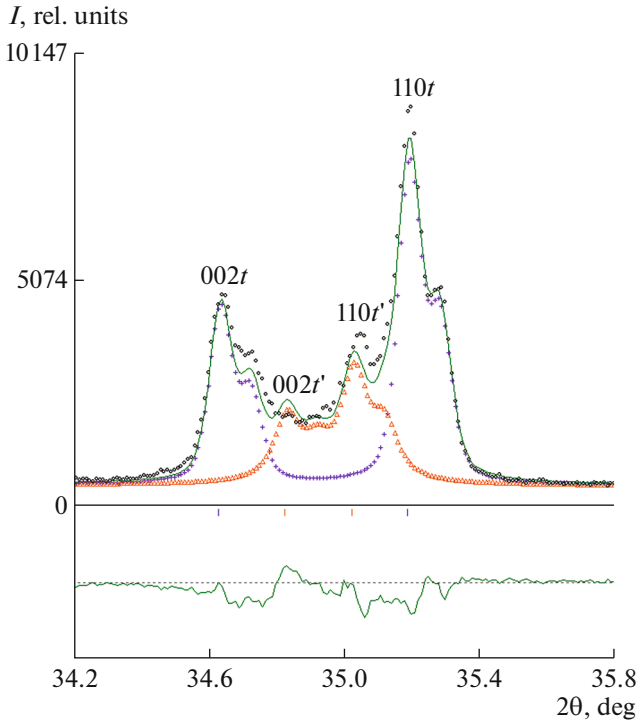

Fig. 1. Part of the diffraction pattern of sample 2 (circles) and the model diffraction patterns of tetragonal form *t* (crosses) and tetragonal form *t*' (triangles); the solid curve is the total spectrum. The difference diffraction pattern is in the bottom.

lowing conditions: temperature 134°C, pressure 2 bar, and exposure 5 h (samples 1h and 2h).

The diffraction patterns of all samples were recorded using an Ultma IV X-ray diffractometer (Rigaku, Japan) under the same conditions: voltage 40 kV; current 30 mA; CuK_α radiation; nickel filter; D/tex high-speed detector; 2.5° Soller slits; 0.5° slit, which limits the incident-beam divergence; detector movement speed 2 deg/min; and step 0.01°. XRD analysis was carried out according to the Rietveld method using the PowderCell [13] and FullProf [14] packages. The parameters in refinement were the zero point with respect to the scattering angle, background component (fifth-order polynomial), scaling factors, profile characteristics of diffraction peaks, unit-cell parameters, atomic coordinates, and isotropic thermal factors. Since insignificant amounts of additives were introduced, the calculations were performed on the assumption of complete occupation of the corresponding crystallographic sites with zirconium atoms.

The element composition of samples 1 and 2 was monitored using an Orbis X-ray spectroscopic microanalyzer (EDAX, United States), which yielded good coincidence between calculated and experimental values. The contents of metals were calculated to be 94.0 at % Zr and 6.0 at % Yb in sample 1 and 93.5 at % Zr, 6.0 at % Yb, and 0.5 at % Nd in sample 2. The corresponding values, determined in the absence of reference, were 94.0 at % Zr, 1.0 at % Hf, and 5.0 at % Yb for sample 1 and 93.0 at % Zr, 1.0 at % Hf, 5.5 at % Yb, and 0.5 at % Nd for sample 2. The microscopic analysis of the surface of samples 1h and 2h was performed in a MIRA3 scanning electron microscope (Tescan, the Czech Republic).

RESULTS AND DISCUSSION

The starting crystallographic data for tetragonal forms *t* and *t*' were taken from [11]. Initially, it was erroneously suggested that samples 1 and 2 contain only form *t*. The presence of two forms *t* and *t*' is clearly demonstrated in Fig. 1, which shows the corresponding diffraction peaks (002) and (110). After preliminary analysis using the PowderCell software, the final refinement was performed within the FullProf program. The graphical refinement results for samples 1 and 2 are shown in Fig. 2, and the main numerical results are presented in Table 1. One can see in Table 1 that the phase compositions of samples 1 and 2 are close: the content of form *t* is about 60 vol %; the rest is form *t*'. The distortion of the initial cubic fluorite cell, which is estimated as the c/a_f ratio, in form *t* exceed that in form *t*'. The refined values of the atomic coordinates and thermal factors of tetragonal forms *t* and *t*', present in samples 1 and 2, are listed in Table 2. Zr and O atoms are characterized by much higher thermal factors in forms *t*' than in forms *t*, which is indicative of atomic disordering at occupation of the corresponding sites (presence of vacancies).

Hydrothermal treatment of the ceramic samples containing the tetragonal ZrO_2 form induces occurrence of the monoclinic modification [8, 9, 15]. This phase was additionally introduced to the considered model before carrying out Rietveld refinement. The crystallographic data were taken from [16]. The refinement results for samples 1h and 2h are shown graphically in Fig. 3, and the main numerical results are presented in Table 1. The monoclinic ZrO_2 (*m*) modification, which is present in samples 1h and 2h, has some specific features. A powder ZrO_2 sample without addition of Yb_2O_3 (maximum firing temperature 950°C) and a ceramic sample of monoclinic ZrO_2 with addition of 1 mol % Yb_2O_3 (sintering temperature 1550°C) were also prepared to determine these features. According to the data of [17], the maximum Yb_2O_3 solubility in ZrO_2 is specifically 1 mol %. The unit-cell parameters of the monoclinic phases, which are present in additionally prepared samples 1h and 2h, are compared with the data from [16] in Table 3. One can see that the unit-cell volume and parameter *a* of the samples after hydrothermal treatment are larger

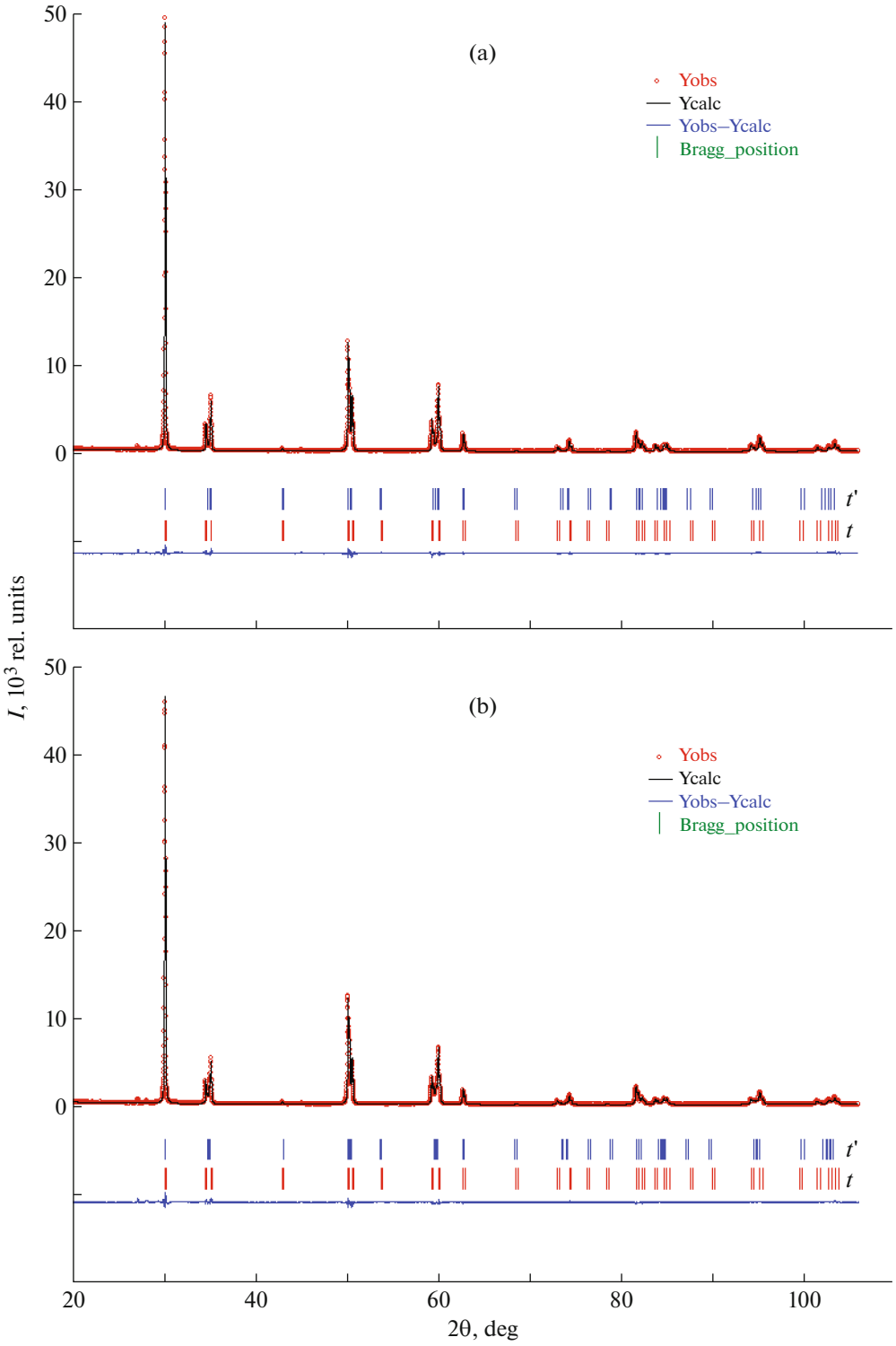

Fig. 2. Graphical results of the Rietveld refinement of the surface structure of samples (a) 1 and (b) 2.

than the corresponding parameters of the additional samples with and without 1% Yb_2O_3. These facts are in agreement with the data of [15] and the suggestion about incorporation of OH^- hydroxyl groups into the crystal structure of monoclinic phases. The refined values of atomic coordinates and thermal factors of the monoclinic phases existing in samples 1h and 2h are listed in Table 4. One can see their good coincidence

Table 1. Main results of Rietveld refinement of the surface structure of ZrO_2 samples

Sample	1	2	1h	2h
R_{wp}, %	7.23	7.42	7.31	7.60
V_t, %	58	59	18	28
R_B, %	3.20	3.42	2.62	2.79
a, c, Å	3.60420(3), 5.17482(5)	3.60394(2), 5.17688(5)	3.60379(7), 5.1711(1)	3.60289(4), 5.17489(8)
c/a_f	1.015	1.016	1.015	1.016
$V_{t'}$, %	42	41	32	38
R_B, %	4.67	3.41	2.94	2.71
a, c, Å	3.6149(1), 5.1549(3)	3.61972(7), 5.1497(1)	3.6133(1), 5.1748(3)	3.6210(1), 5.1605(2)
c/a_f	1.008	1.005	1.013	1.009
V_m, %			50	34
R_B, %			5.99	5.51

a_f is the parameter of cubic fluorite cell, calculated according to the formula $a_f = a\sqrt{2}$ [11]; c/a_f is the distortion of the initial cubic fluorite cell; and V_t, $V_{t'}$, and V_m are, respectively, the volume contents of the t, t', and monoclinic forms.

Table 2. Refined atomic coordinates and isotropic thermal factors of the tetragonal ZrO_2 forms

Atom, parameter	Sample			
	1	2	1h	2h
Form t				
Zr, B_{iso}, Å^2	1.05(3)	1.201(9)	0.31(2)	0.27(2)
O, z	0.459(1)	0.458(1)	0.460(1)	0.466(1)
O, B_{iso}, Å^2	2.07(7)	2.19(7)	0.31(2)	0.78(9)
Form t'				
Zr, B_{iso}, Å^2	4.03(8)	3.46(2)	3.14(8)	3.02(4)
O, z	0.478(4)	0.49(1)	0.477(7)	0.464(3)
O, B_{iso}, Å^2	5.9(2)	5.8(1)	4.4(3)	4.9(2)

Both t and t' forms are characterized by sp. gr. $P4_2/nmc$ (no. 137). Zr and O atoms occupy the Wyckoff positions 2a (3/4, 1/4, 3/4) and 4d (1/4, 1/4, z), respectively.

and good correspondence with the data of [16]. Another feature of these monoclinic phases is that the relative intensities of the diffraction peaks are inconsistent with the data from the PDF2 database (in particular, card 83-940). This inconsistency is clearly demonstrated in Fig. 4. The $(\bar{1}11)$ peak is much stronger than the (111) peak of the monoclinic phase of sample 1h, while in the case of powder ZrO_2 sample

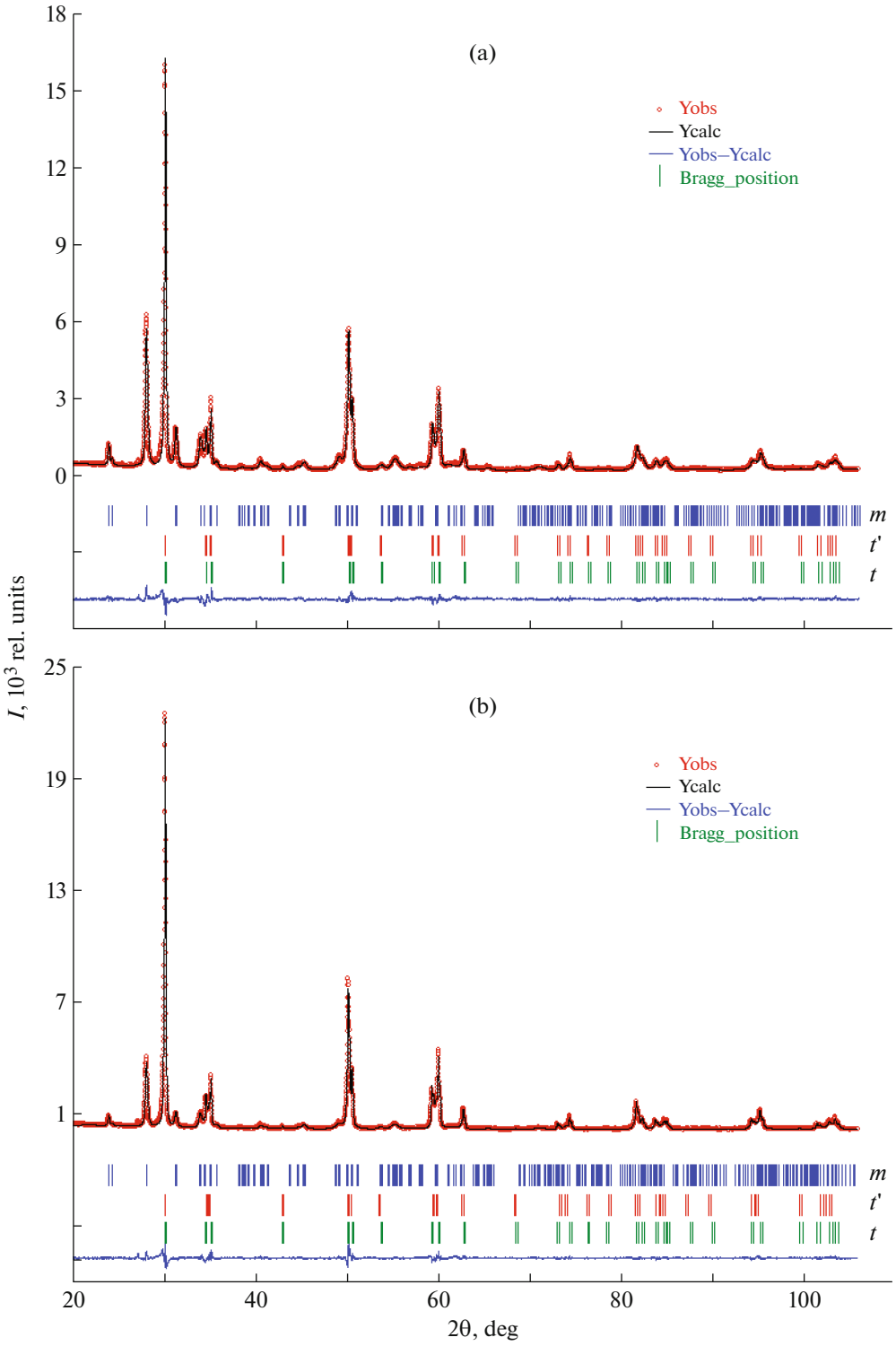

Fig. 3. Graphical results of the Rietveld refinement of the surface structures of samples (a) 1h and (b) 2h.

these peaks have close intensities. The same situation is also observed for the (011) and (110) peaks. These phenomena are due to the lamellar shape of the *m*-ZrO_2 crystals formed during hydrothermal treatment. The plates are elongated in the [111] direction and have developed {001} faces. The corresponding corrections were introduced into the refined Rietveld model, which made it possible to reach low reliability factors

Table 3. Unit-cell parameters of the monoclinic ZrO_2 phases

Sample	1h	2h	ZrO_2 (1 mol % Yb_2O_3)*	ZrO_2**	[16]
a, Å	5.1732(5)	5.1737(8)	5.1598(1)	5.14605(6)	5.1451(3)
b, Å	5.2066(4)	5.2012(6)	5.2139(1)	5.20952(7)	5.2023(4)
c, Å	5.3318(3)	5.3337(3)	5.3171(1)	5.31476(7)	5.3219(4)
β, deg	99.104(4)	99.071(7)	99.233	99.2026(9)	99.15(3)
V, Å^3	141.8	141.7	141.2	140.6	140.6

* Sintering temperature of 1550°C.
** Firing temperature of 950°C.

Table 4. Refined atomic coordinates and isotropic thermal factors of the monoclinic ZrO_2 phases

Atom	Parameter	Sample 1h	Sample 2h	[16]
Zr	x	0.2728(4)	0.2708(7)	0.2760(5)
	y	0.0354(3)	0.0334(6)	0.0401(4)
	z	0.2103(3)	0.2104(4)	0.2091(4)
	B_{iso}, Å^2	1.40(6)	2.74(9)	0.461(4)
O1	x	0.058(2)	0.044(3)	0.072(3)
	y	0.381(2)	0.393(3)	0.333(2)
	z	0.402(1)	0.409(1)	0.347(2)
	B_{iso}, Å^2	2.2(4)	2.74(9)	0.461(4)
O2	x	0.409(2)	0.403(3)	0.449(3)
	y	0.835(1)	0.848(2)	0.758(2)
	z	0.472(2)	0.483(3)	0.476(4)
	B_{iso}, Å^2	0.4(2)	2.74(9)	0.461(4)

(Table 1). The monoclinic phase of sample 2h also exhibits this specific feature. It was reported previously [18, 19] that the m-ZrO_2 crystals formed as a result of the hydrothermal treatment are elongated in the [111] direction and have a lamellar or needle-like shape. It should also be noted that the diffraction peaks corresponding to the monoclinic phases of samples 1h and 2h are broadened in comparison with the peaks of tetragonal forms. This broadening may be due to the small size of the coherent-scattering region, which is usually related to the geometric size of particles. To verify this suggestion, calculations for the strongest $(\bar{1}11)$ peak of the monoclinic phases of samples 1h and 2h were performed using the WinFit program [20]. A ceramic ZrO_2 sample with addition of 1 mol % Yb_2O_3, sintered at 1550°C, was used as a reference sample. The coherent-scattering regions were 83 and 87 nm in size, respectively.

The results of scanning electron microscopy are presented in Fig. 5. The chosen portion is characteristic of samples 1h and 2h. It can be seen that the surface of sample 1h after hydrothermal treatment is irregular: it has ridges and valleys, formed as a result of partial dissolution of the surface layer. The ceramic grains are

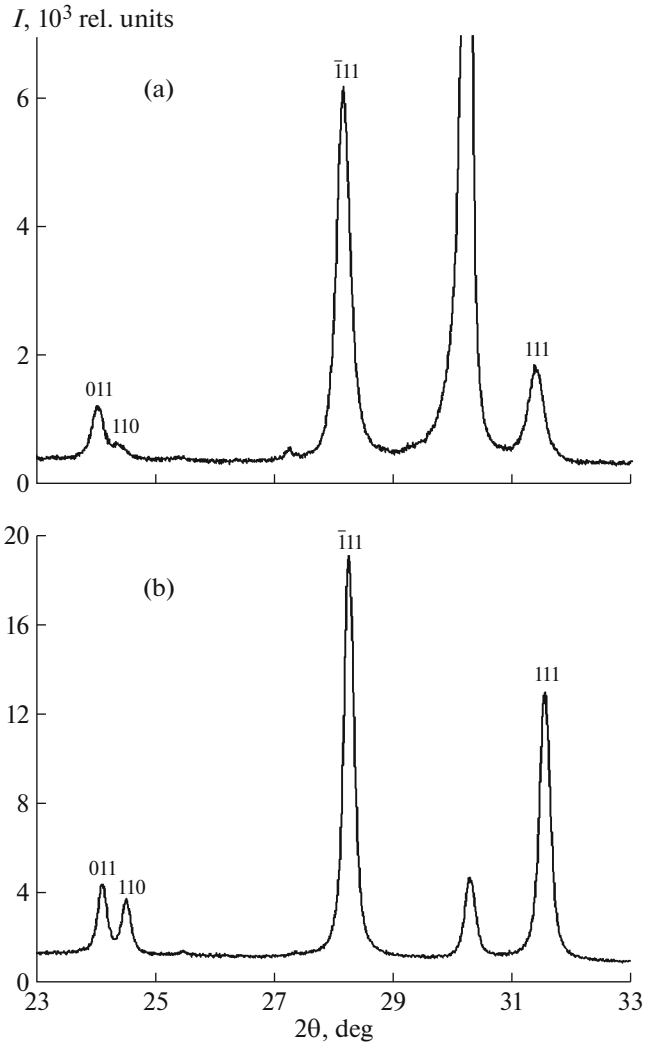

Fig. 4. Parts of the diffraction patterns of (a) sample 1h and (b) powder monoclinic ZrO_2 modification, synthesized at 950°C. The reflections of the monoclinic modification are indexed.

mainly about 0.5 μm in size; however, individual grains reach 3–5 μm. This grain size is characteristic of ZrO_2 ceramics stabilized into the tetragonal form after sintering at 1500°C [21]. No ZrO_2 crystals of monoclinic modification were observed at the chosen magnification.

CONCLUSIONS

The XRD analysis according to the Rietveld method showed that, after sintering at 1550°C, the ceramic samples, consisting of yttrium oxide with addition of ytterbium oxide (3 mol %) and oxides of ytterbium (3 mol %) and neodymium (0.25 mol %), contain two tetragonal ZrO_2 forms (*t* and *t*'). The phase composition of the surface changes, and dissolution and crystallization processes of the monoclinic ZrO_2 modification occur during hydrothermal treatment. Two tetragonal forms (*t* and *t*') and the monoclinic phase (*m*) are present on the sample surface. The monoclinic crystals are shaped as plates elongated in the [111] direction, with the developed {001} faces. Addition of neodymium oxide slows down the monoclinic-phase formation.

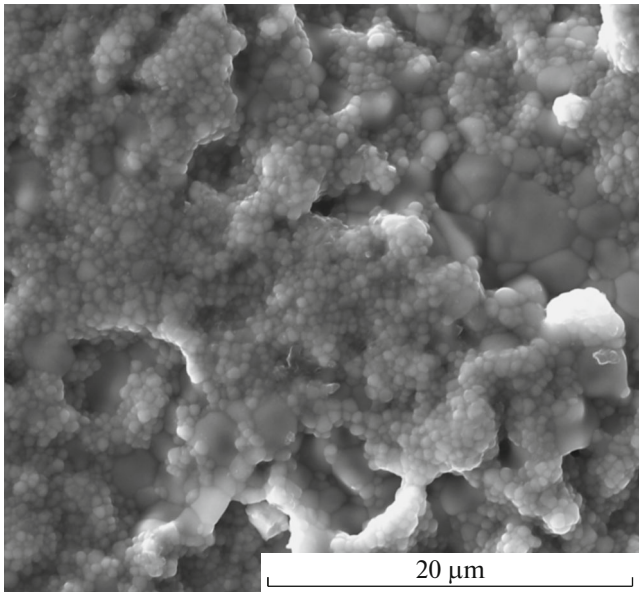

Fig. 5. General view of the surface of sample 1h after hydrothermal treatment.

CONFLICT OF INTEREST

The authors declare that they have no conflicts of interest.

REFERENCES

1. J. Chevalier, A. Liens, H. Reveron, et al., J. Am. Ceram. Soc. **103**, 1482 (2020). https://doi.org/10.1111/jace.16903
2. C. Piconi and G. Maccauro, Biomaterials **20**, 1 (1999). https://doi.org/10.1016/S0142-961(98)00010-6
3. J. Chevalier, Biomaterials **27**, 535 (2006). https://doi.org/10.1016/j.biomaterials.2005.07.034
4. J. R. Kelly and I. Denry, Dental Mater. **24**, 289 (2008). https://doi.org/10/1016/j/dental.2007.05.005
5. L. Borshers, M. Stiesch, F.-W. Bach, et al., Acta Biomater. **6**, 4547 (2010). https://doi.org/10/1016/j.actbio.2010.07.025
6. M. Cattani-Lorente, S. Scherrer, P. Ammann, et al., Acta Biomater. **7**, 858 (2011). https://doi.org/10.1016/j.actbio.2010.09.020
7. P. Kohorst, L. Borchers, J. Strempel, et al., Acta Biomater. **8**, 1213 (2012). https://doi.org/10.1016/j.actbio.2011.11.016

8. L. I. Podzorova, S. A. Titov, A. A. Il'icheva, et al., Materialovedenie, No. 7, 52 (2015).
9. L. I. Podzorova, A. A. Il'icheva, N. A. Mikhailinoi, et al., Perspekt. Mater., No. 2, 27 (2017).
10. M. Yashima, N. Ishizawa, and M. Yoshimura, J. Am. Ceram. Soc. **76**, 641 (1993). https://doi.org/10.1111/j.1151-2916.1993.tb03654.x
11. M. Yashima, S. Sasaki, M. Kakihana, et al., Acta Crystallogr. B **50**, 663 (1994). https://doi.org/10.1107/S0108768194006257
12. M. Yashima, M. Kakihana, and M. Yoshimura, Solid State Ionics **86–88**, 1131 (1996). https://doi.org/10.1016/0167-2738(96)00386-4
13. W. Kraus and G. Nolze, J. Appl. Crystallogr. **29**, 301 (1996). https://doi.org/10.1107/S0021889895014920
14. J. Rodriguez-Carvajal, Physica B **192**, 55 (1993). https://doi.org/10.1016/0921-4526(93)90108-1
15. M. Yoshimura, T. Noma, K. Kawabata, and S. Somiya, J. Mater. Sci. Lett. **6**, 465 (1987). https://doi.org/10.1007/BF01756800
16. M. Winterer, R. Delaplane, and R. McGreevy, J. Appl. Crystallogr. **35**, 434 (2002). https://doi.org/10.1107/S0021889802006829
17. M. Gonzalez, C. Moure, J. R. Jurado, and P. Duran, J. Mater. Sci. **28**, 3451 (1993). https://doi.org/10.1007/BF01159821
18. L. Kumari and W. Z. Li, Cryst. Growth Des. **9**, 3874 (2009). https://doi.org/10.1021/cg800711m
19. H. Nishizawa, N. Yamasaki, K. Matsuoka, and H. Mitsushio, J. Am. Ceram. Soc. **65**, 343 (1982). https://doi.org/10.1111/j.1151-2916.1982.tb10467.x
20. S. Krumm, Mater. Sci. Forum. **228–231**, 183 (1996). https://doi.org/10.4028www.scientific.net/MSF.228-231
21. L. Hallmann, P. Ulmer, E. Reusser, et al., J. Eur. Ceram. Soc. **32**, 4091 (2012). https://doi.org/10.1016/j.jeurceramsoc.2012.07.032

Translated by Yu. Sin'kov